Development of An Adaptive Moving Overset Grid Technique for CAA

Joonseok Lee*, Chi-Hoon Cho**, Duck-Joo Lee**

* Renault Samsung Motors CO.,LTD, Korea
(Tel : +82-31-289-7375, E-mail: joonseok.lee@renaultsamsungM.com)
** Division of Aerospace Engineering, KAIST, Korea

Abstract: Composing high quality grid is one of the most critical issue in using of CFD(Computational Fluid Dynamics) technique. In this paper, an adaptive moving overset grid technique has been developed which can be applied not only to conventional CFD technique but also to CAA(Computational AeroAcoustics) technique needing higher order of accuracy. Up to now days, the overset grid has been used as body fitting grid which is attached to moving body or to separated body usually. But in this research one of the sub grids is used as vortex fitting grid, so that great amount of mesh size could be reduced for conserving a vortex which has high gradient characteristics. Finally 2D blade-vortex interaction phenomena is simulated with 2D Euler equation and high order compact finite difference scheme and 4th order Runge-kutta methods are used as numerical scheme. The 4th order Lagrange interpolation has been applied for domain connectivity.

Keywords: CAA, overset grid, compact scheme, Lagrange interpolation.

1. INTRODUCTION

This article describes the development of the adaptive moving overset grid technique for CAA(Computational Aero-Acoustics) which is a branch of CFD mainly focusing on sound radiating and scattering phenomena. Although the overset grid has many outstanding strong points when employed to complicate shaped-body or multi-body related problem, there have been not many CAA research using it. CAA needs higher order of accuracy numerical method compared to conventional CFD. That means high order interpolation should be applied also when interpolation is conducted. Or the acoustic wave may be not conserved and dissipated when it passes through the overlapped region. In this research, high order Lagrange interpolation method is suggested as a solution. From the error analysis, the order of interpolation has been determined and the interpolation constants are obtained by Newton's method for minimizing the error. The applicability of this interpolation method has been validated successfully with BVI(Blade vortex interaction) problem. And finally it is confirmed through this research that high order numerical schemes which have been used for CAA problem before work well with overset grid technique also.

2. NUMERICAL METHOD

2.1 Governing equation

As a governing equation, 2D Euler equation (Eq.1) transformed to computational space from physical space is used.

$$\frac{\partial \hat{Q}}{\partial \tau} + \frac{\partial \hat{E}}{\partial \xi} + \frac{\partial \hat{F}}{\partial \eta} = 0 \qquad \text{Eq.(1)}$$

$$\hat{Q} = \frac{Q}{J}, \quad \hat{E} = \frac{1}{J}(\xi_t Q + \xi_x E + \xi_y F), \quad \hat{F} = \frac{1}{J}(\eta_t Q + \eta_x E + \eta_y F)$$

$$Q = \begin{bmatrix} \rho \\ \rho u \\ \rho v \\ \rho e_t \end{bmatrix}, \quad E = \begin{bmatrix} \rho u \\ \rho u^2 + p \\ \rho u v \\ (\rho e_t + p)u \end{bmatrix}, \quad F = \begin{bmatrix} \rho v \\ \rho u v \\ \rho v^2 + p \\ (\rho e_t + p)v \end{bmatrix}$$

2.2 Numerical scheme

For simulating the acoustic properties, the order of numerical scheme should be high enough and here the 'high order compact finite difference scheme'[1] is applied as spatial difference scheme. This scheme can keep up to 10th order accuracy, but in this research, 4th order of accuracy form is used and the margins are used for optimizing the constant used in Eq.2.

$$\beta f'_{i-2} + \alpha f'_{i-1} + f'_i + \alpha f'_{i+1} + \beta f'_{i+2} = a\frac{f_{i+1} - f_{i-1}}{2\Delta x} + b\frac{f_{i+2} - f_{i-2}}{4\Delta x} + c\frac{f_{i+3} - f_{i-3}}{6\Delta x} \qquad \text{Eq.(2)}$$

$$a = 0.6431406736919156$$
$$b = 0.2586011023495066$$
$$c = 0.0071409534797973$$
$$\alpha = 0.5862704032801503$$
$$\beta = 0.0954953355501705$$

As a time difference schemes corresponding to the 4th order spatial difference scheme, Runge-kutta method which is the 4th order of accuracy also is used. When one apply center scheme, the dispersion may be appeared if there are sudden characteristic change such is shock wave. To reduce this kind of error, Kim and Lee's ANAD(Adaptive nonlinear artificial dissipation) model[2] is used. And as a non reflecting boundary condition, also Kim and Lee's GCBC(Generalized characteristic boundary condition) is applied[3].

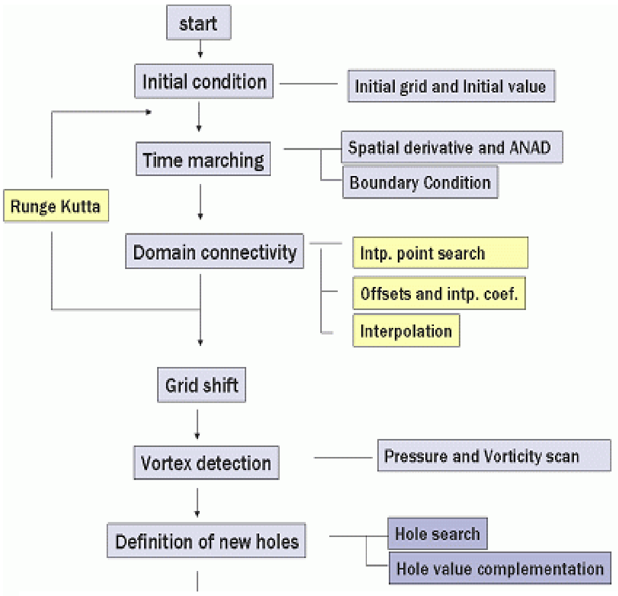

Fig. (1) The overall process

2.3 Calculation process

The fig.(1) shows the overview of calculation process of this research. At very first, the calculations of the 'Runge – kutta method's first loop are conducted at each sub grids independently with initial condition. During that, the spatial derivatives are calculated and the ANAD and the GCBC model are taken in. After then, the calculation results for each sub domains are exchanged each other with high order interpolation method. This domain connectivity should be conducted for every 'Runge-kutta' step. In case of moving grid system, grid shifting is happen after each time marching step. In this research one of the sub domains is designed to contain a moving vortex from start to end, so the vortex detection algorithm is needed to make the sub domain move to the place where vortex is. As a last stage for a time step, the holes should be defined newly for the calculation of next time step. These stages would be repeated until one get the final result.

3. OVERSET GRID TECHIQUE

The overset grid technique needs two additional algorithms compared to unique grid type technique in a wide sense. The first thing is domain connectivity which is done by interpolation. The second thing is hole treatment for excluding the hole points from the time marching calculation.

3.1 Domain connectivity

The very first step for interpolation is searching a donor points which should be the nearest ones from the receiver point. In this research, the AIS(Alternative Index searching) method[4] is used with modified form. The AIS method starts with defining a initial point arbitrary. And the next candidate donor point is determined by the sign of dot product between vectors which are overlapped with grid stencil and the vector from candidate point to receiver point. By repeating this inspection, the position of the candidate point would approach to receiver point (and to final correct donor point also) with diagonal direction. The 'diagonal direction' means the number of inspections could be decreased compare to the 'stencil direction' and we could save the calculation resource.

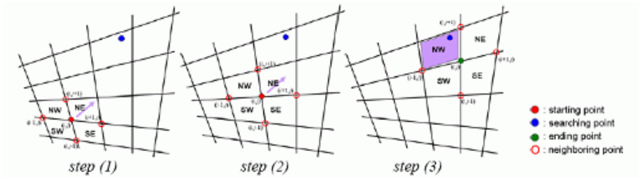

Fig. (2) Alternating Index Searching method [4]

The fig.(3) is a schematic of the single dimensional interpolation model. The black body points are donor points and the hollow one means a receiver point. The distances between each donor points are equal as unit length because this model is placed in the computational space after being transformed from the physical space.

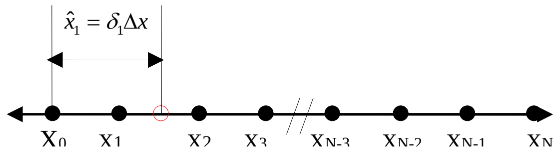

Fig. (3) A schematic of 1D interpolation model

The number of donor points corresponding to a receiver point determines the interpolation order of accuracy. A small number of donor points not only makes the algorithm simple and the calculation speedy but also the interpolation error big and the quality of result low. To conserve the high gradient properties of a vortex when it is passes from a sub domain to other sub domain, interpolation error should be very small. To determine the level of acceptable error level, An error analysis is conducted with respect to various number of donor points. The generalized 1D Lagrange interpolation method is expressed as Equation (3). The number of donor point is N.

$$\hat{f}(\hat{x}) = \sum_{j=0}^{N-1} R_j f(x_j) \qquad \text{Eq.(3)}$$

R_j : Interpolation coefficient $R_j = R_j(\delta_j)$

$\hat{f}(\hat{x})$: unknown value of receiver point.

$f(x_j)$: known values of donor points.

For Fourier error analysis, let $f(x) = \exp(i\alpha x)$.

The local error for specific wave number α, is Equation(4) and the integrated error for a unit wave number domain is Equation(5).

$$E_{local} = \left| e^{i\delta_c \alpha} - \sum_{j=0}^{N-1} R_j e^{ij\alpha} \right|^2 \qquad \text{Eq.(4)}$$

$$E_{\text{int}} = \int_0^1 \left| e^{i\delta\,\alpha} - \sum_{j=0}^{N-1} R_j e^{ij\alpha} \right|^2 d\alpha \qquad \text{Eq.(5)}$$

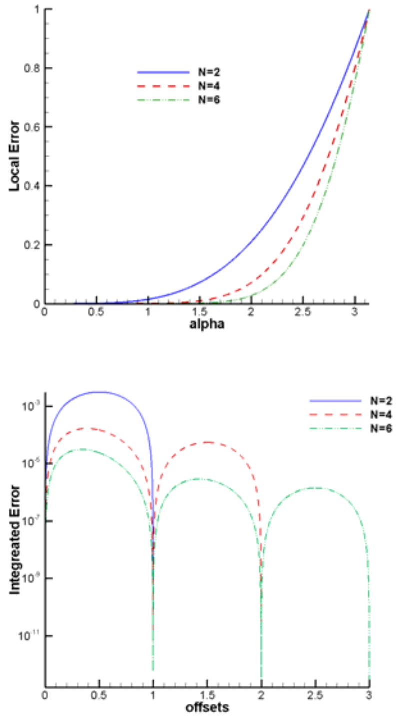

Fig.(4) Local error(top) and Integrated error(bottom)

The local and integrated error are figured out as fig.(4). Regarding the magnitude of the objective acoustic wave, 4^{th} order of accuracy (N=4) is selected as a proper interpolation method and applied to every interpolation in this research. To practical use of its strength in error, the positions of the selected donor points should not be offset to specific direction which means the receiver point should be located between the 2^{nd} and 3^{rd} donor points in case of N=4.

The relation between offsets δ and the interpolation constant is expressed as Eq. (6). The offset represent the relative distance between the receiver point and a donor point. The offset would be obtained from cyclic calculation with Newton method. The constants for 2D problem can be determined by simply expanding the 1D problem.

$$\alpha_j = \frac{(-1)^{N+j-1}}{[N-(j+1)]!\,j!}$$

$$R_j = \alpha_j \prod_{\substack{i=0 \\ i \neq j}}^{N-1} (\delta_1 - i) \qquad \text{Eq.(6)}$$

3.2 Grid size effect for interpolation

To find out the acceptable max ratio of grid size for conserving the vortex between the background grid and the vortex containing grid, an validation test is conducted as follow. The test system is consist of a large rectangular background grid and a dense square grid containing a vortex. The number of grid points of square grid is restricted as 36points per radius of the vortex when the size of background grid is changed as 8:1, 10:1, 20:1, 30:1 and 40:1 in terms of ratio of grid size. 10:1 means the size of a cell in the background grid is 10 times larger than that of vortex containing grid. The vortex whose radius is 0.04 and the small grid are located at (-4,0) initially and would move to (4,0) with free stream. The speed of free stream is Mach 0.5. After the movement, the level of conservation of the vortex can be a gauge for determining the performance of each cases.

Fig. (5) shows that in case of 8:1, 10:1 and 20:1, the y-direction velocity is almost same with exact solution. With this result one can conclude there is no problem to increase the ratio of the cell sizes up to 20:1. That means one can use only quarter number (2D) of grid points for background grid compared to the case of 10:1.

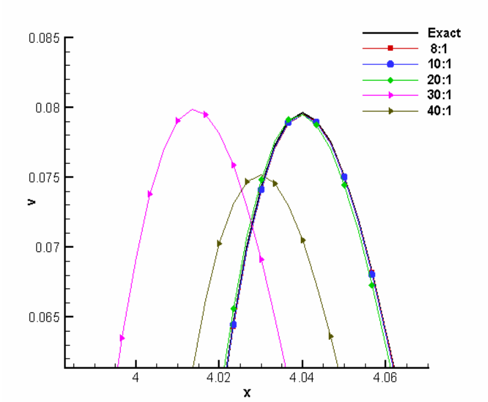

Fig.(5) Y-direction velocity for the vortex

3.3 Hole points treatment

At the overlapped region some grid points of one sub grid could be located on the another grid's body where the objective fluid is not exist. This kind of points are called hole and should be excluded from the calculation to avoid unphysical result. This will be done by modifying the LHS and RHS of the derivative matrix as follow(Fig(6)).

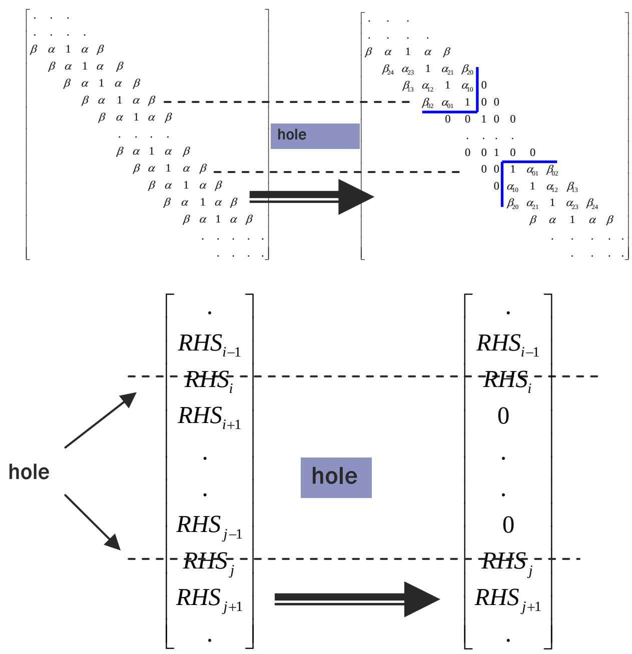

Fig.(6) Matrix modification for the hole, LHS(top) and RHS(bottom)

4. VALIDATION

4.1 Moving vortex

This problem is for the validation of the numerical schemes and overset grid methods developed together. The grids system is consist of two sub grid, one is the background grid with hole region at the center and the other is a sine function shaped grid which is covering the hole region. At first the vortex located at (-5,0) and will move to right side with a free stream whose speed is Mach 0.5. The vortex will move on the background grid first and be transferred to sine shaped grid and will be on the background grid again after passing through the hole region. Fig.(7) shows the grid system and initial position of the vortex for this problem.

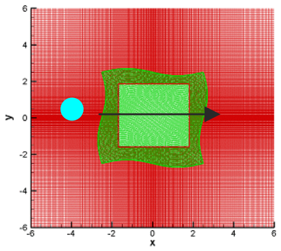

Fig. (7) The overset grid system for a moving vortex

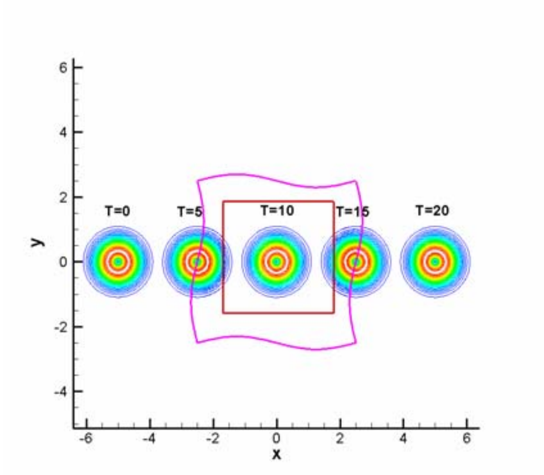

Fig. (8) The velocity contour for moving vortex

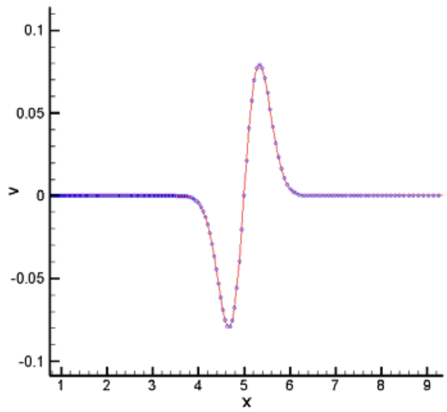

Fig. (9) Y-direction velocity comparison at T=20, single grid(-) vs. overset grid(.)

According to the overall velocity contours in Fig.(8), the shape of vortex is almost same between initial state(T=0) and after transfer(T=20). Fig.(9) shows the comparison of the y-direction velocity at the vortex centerline between two vortexes, one was moved on single grid from initial to final and the other is transferred vortex which is passed from one grid to other twice by interpolation. The former one could be considered as reference solution. The y-direction velocity is perfectly matched each other. That means there is little dissipation during the interpolation process and the numerical method used in this research is useful for vortex related problem.

4.2 Blade-vortex interaction

To simulate BVI phenomenon three different kinds of sub grids are used together like fig.(10). The first one is the large background grid which is Cartesian type and the second one is C-grid surrounding NACA0012 airfoil. The last third one is the small rectangular grid which would keep up with the moving vortex. Let us call the grids as background grid, airfoil grid and vortex grid respectively. Usually, the Blade-vortex interaction problem needs very dense mesh at the vortex path from start to end even the vortex stay there not so long time. However, there is no this kind of waste here because of the vortex grid. The total number of grid points is not so big even though the grid is very dense because its overall coverage is small. That is one of the most charming benefit for applying overset grid to a vortex related problem.

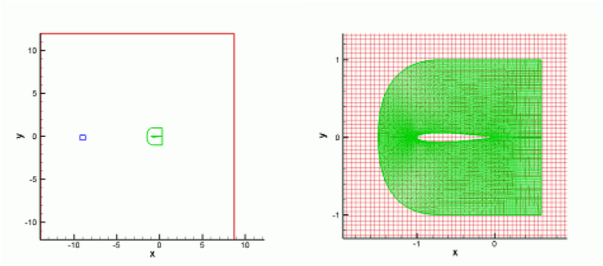

Fig. (10) The overset grid system for a BVI.

Initially the center of vortex and the vortex grid are located at (-6, 0) when the leading edge of the airfoil is located at (-1, 0). There is no angle of attack and the Scully model is used as the vortex model.

$$\text{Scully model} :: \left(V_\theta = \frac{\Gamma}{2\pi r_c} \frac{r/r_c}{(1+(r/r_c)^2)} \right) \qquad \text{Eq.(7)}$$

4.2.1 $M_\infty = 0.8, \Gamma = 0.16, Y_v = -0.26, r_c = 0.05$

Two similar but different cases are analyzed here. In case of the first problem, there is a small interaction distance between the center of vortex and the chord line of the airfoil. And because of the fast free steam, it is Mach 0.8, a shock would appear near the airfoil.

For the first problem, initial steady state is obtained using only background grid and airfoil grid. Fig.(11) is the pressure contour in steady state long time after the free stream starts. The pressure coefficient distribution on the airfoil surface is well matched with the results of other researchers, Oh[5] and Pulliam[6]. (Fig. (12))

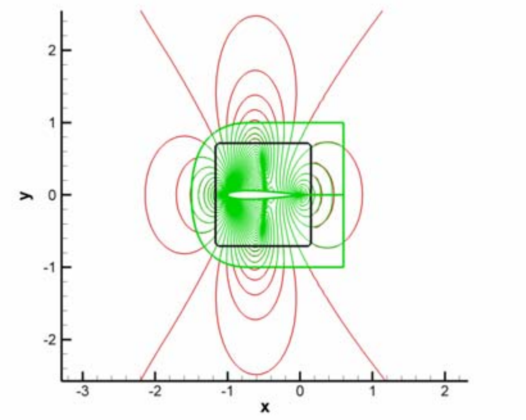

Fig. (11) Pressure contour near the airfoil (M=0.8).

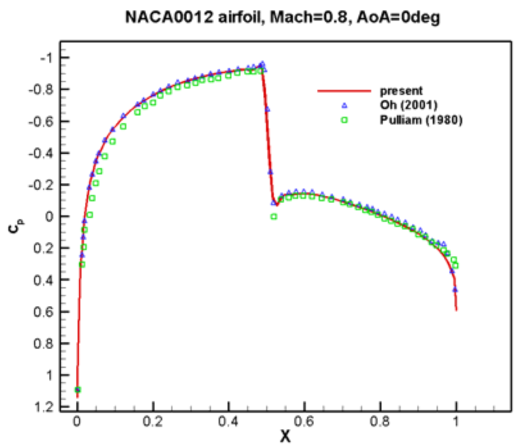

Fig. (12) Pressure coefficient on the airfoil surface (M=0.8).

With this initial condition, a vortex and the third vortex grid is embedded at 5c before position from the leading edge. Fig. (13) shows the pressure contour sequence corresponding to the position of the vortex. The parts surround by black line are hole region where all points inside are hole points. The position and shape of hole region change from time to time according to position of the vortex.

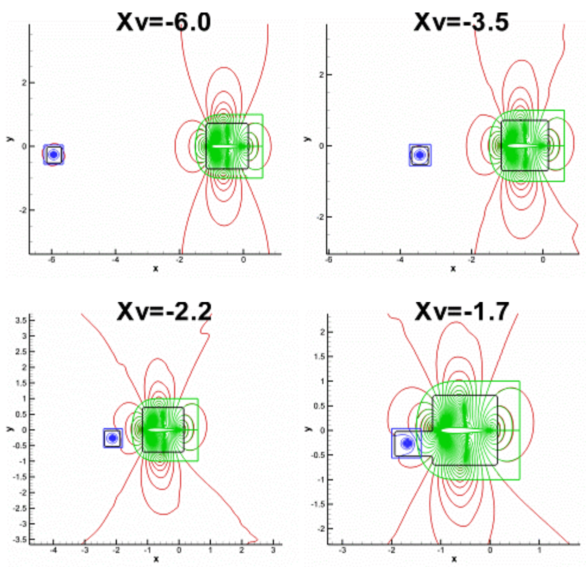

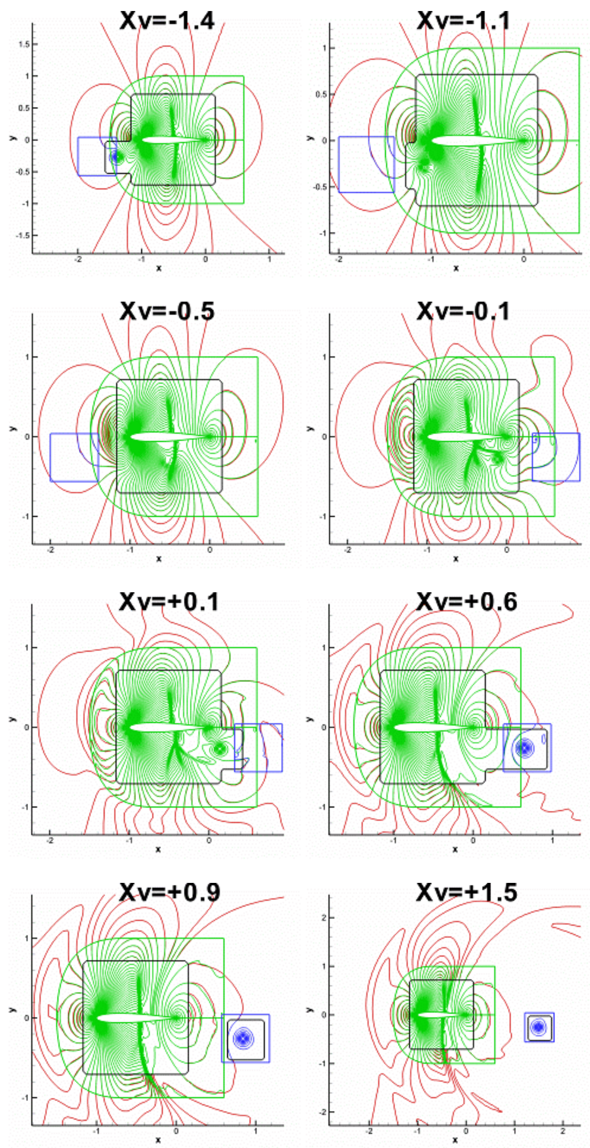

Fig. (13) Sequence of pressure contour (M=0.8)

One can observe that even after passing through the shock region, the shape of vortex recovered clearly. The lift variation of the airfoil obtained here agree well with other researcher's results[7,8].

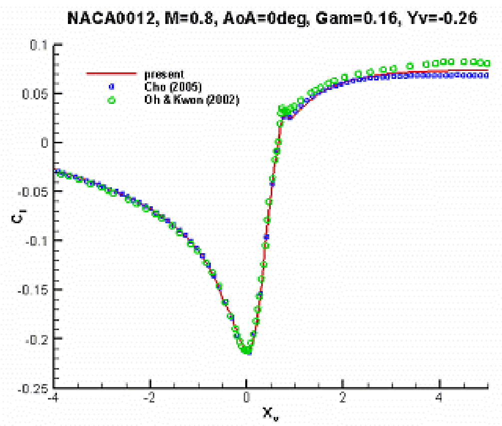

Fig. (14) Lift variation

4.2.2 $M_\infty = 0.5, \Gamma = 0.13, Y_v = 0.0, r_c = 0.05$

At second case, there is no interaction distance between the vortex and leading edge and the free stream speed is Mach 0.5. This problem is for observing the behavior of the acoustic wave which is radiated from the leading edge. The overlooks of sequence shots is not so difference from case 1.(Fig. (15)). But the radiating acoustic wave is very clear and the wave also pass the interpolation boundary smoothly without any discontinuation like the vortex.

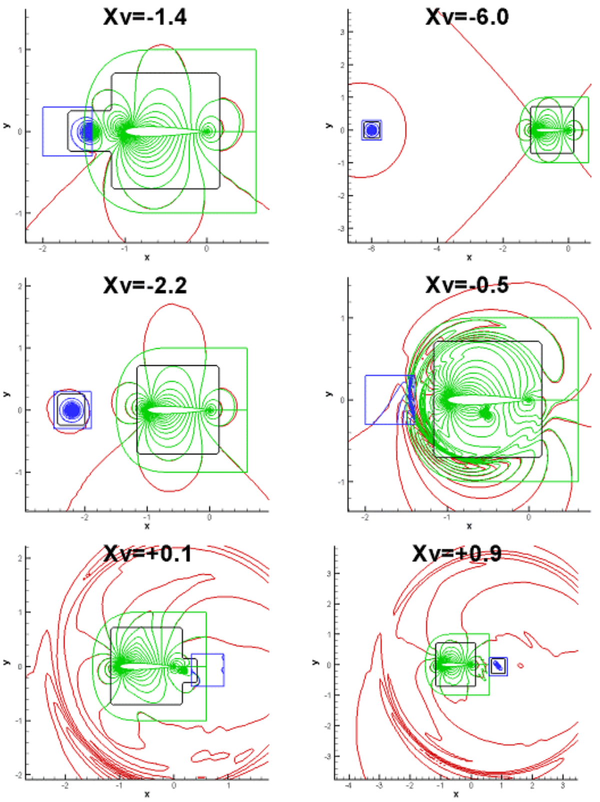

Fig. (15) Sequence of pressure contour (M=0.5)

Fig.(16) is the directivity of RMS value for acoustic pressure at the moment when the center of vortex coincide with leading edge. The values are obtained on the circle which radius is 5c from the leading edge. The overall pattern of present result agree well with Cho[22]'s result.

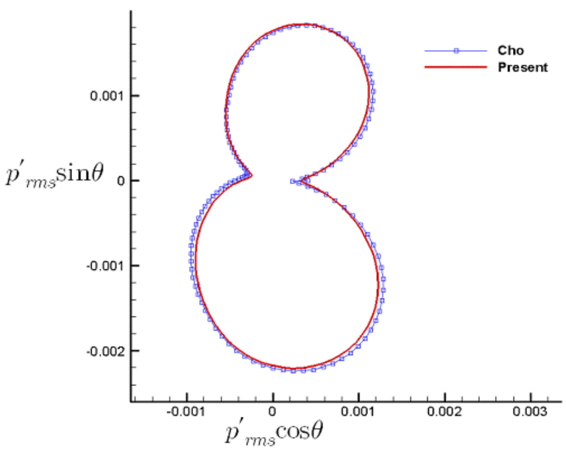

Fig. (16) Sequence of pressure contour (M=0.5)

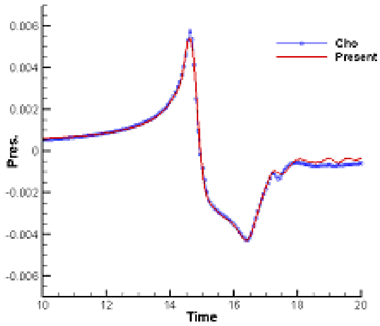

Fig. (17a) acoustic pressure at (-1 , 5)

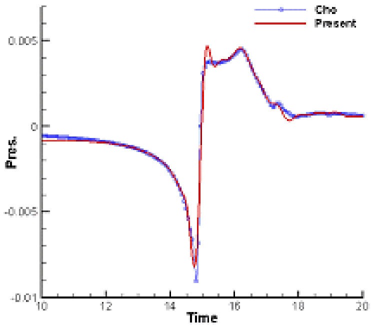

Fig. (17b) acoustic pressure at (-1 , -5)

Because of the circulation of the vortex, the pressure pattern is not symmetric and the pressure has a maximum value at vertical below position from the leading edge.

Two figure above(fig.(17) are acoustic pressure value according to the time at (-1, 5) and (-1, -5) each. They have max value at T=15 and that tells us the acoustic wave occurred at T=10, the moment the vortex impinge the leading edge. The trend is very similar with Cho's result. He used same numerical scheme but blocked grid instead of overset grid.

REFERENCES

[1] J. W. Kim, *"Optimised Boundary Compact Finite Difference Schemes for Computational Aeroacoustics,"* 12th AIAA/CEAS Aeroacoustics conference, Cambridge, Massachusetts, 8-10, may, 2006.

[2] J. W. Kim and D. J. Lee, *"Adaptive Nonlinear Artificial Dissipation Model for Computational Aeroacoustics,"* AIAA Journal, vol.39, No.5, pp810-818, 2001

[3] J. W. Kim and D. J. Lee, "*Generalized Characteristic Boundary conditions for Computational Aeroacoustics, Part 2,"* AIAA Journal, Vol.42, No.1, pp47-55, 2004

[4] C. Yang, *"Numerical analysis of helicopter noise using alternating index searching algorithm"*, The 9th WESPAC, Seoul, Korea, 26-28 Jun, 2006

[5] W. S. Oh, *"Analysis of Unsteady Flows Past Airfoils on Unstructured Adaptive Meshes,"* Ph.D. Thesis, KAIST, 2001

[6] T. H. Pulliam and J. L. Steger, "*Implicit Finite-Difference Simulations of Three-Dimensional Compressible Flow*," AIAA Journal, vol.18, No.2,1980

[7] C. H. Cho, personal contact, 2006

[8] W. S. Oh, J. S. Kim and O. J. Kwon, *"Numerical Simulation of Two-Dimensional Blade-Vortex Interactions Using Unstructured Adaptive Meshes,"*

AIAA Journal, Vol.40, No.3, 2002